Engineering and Technology Journal
Journal homepage: https://etj.uotechnology.edu.iq

Optimizing parameters for fiber laser cutting stainless steel 201 to improve kerf width quality

Anwar H. Zabon[a]*, Tahseen F. Abbas[b], Aqeel S. Bedan[a]

[a] Production Engineering and Metallurgy Dept., University of Technology-Iraq, Alsinaa street, 10066 Baghdad, Iraq.
[b] Aeronautical Technical Engineering Dept., Technical Engineering College, Al-Farahidi University, Iraq.
*Corresponding author Email: pme.22.04@grad.uotechnology.edu.iq

HIGHLIGHTS

- Laser cutting parameters were investigated for their effect on the cut quality of stainless steel 201.
- A comprehensive study was conducted on the combined effect of V, Pu, F, FP, and P on kerf width.
- ANOVA was used to assess the statistical significance of each cutting parameter.
- Correlation models were developed to find optimal laser cutting settings for better-cut quality.
- Laser power and focal position have the greatest impact on kerf quality.

Keywords:
Fiber laser; top kerf width; bottom kerf width; RSM; SST 201.

ABSTRACT

This study investigates the laser cutting of stainless steel 201 using the Response Surface Methodology with a 32-run experimental design (L32). The responses are top and bottom kerf width, while laser power, cutting speed, frequency, focal position, and gas pressure are selected as input process parameters. A comprehensive statistical analysis, including analysis of variance, main effect plots, residual plots, and interaction plots, was conducted to assess the significance and contribution of each parameter. The ANOVA results for TKW and BKW confirmed the statistical significance of all machining variables. For BKW, laser power had the highest influence (72%), followed by focal position (17%), frequency (8%), gas pressure (2%), and cutting speed (1%). Similarly, for TKW, laser power contributed the most (61%), followed by focal position (19.8%), gas pressure (4.5%), cutting speed (3.8%), and frequency (2.7%). The findings highlight the dominant role of laser power and focal position in determining kerf quality. This study's main contribution is pinpointing the ideal laser cutting parameters for reducing kerf width, which improves precision and efficiency in stainless steel 201 cutting. The findings serve as a valuable reference point for enhancing laser-cutting processes in industrial applications.

1. Introduction

Laser cutting is a highly advanced machining process that utilizes heat energy to cut materials without direct contact with the workpiece. The term "laser" stands for "Light Amplification by Stimulated Emission of Radiation" and refers to a device that generates a coherent, monochromatic light beam. Due to their spatial coherence, lasers can be precisely focused on a small area, making them highly suitable for various industrial and medical applications. In manufacturing, lasers are widely used for welding, drilling micro-holes, and cutting thick metal sheets with high precision and tight tolerances. Since laser cutting does not require physical tools, it eliminates mechanical wear and tool degradation, making it advantageous over traditional machining methods [1,2]. Laser cutting can be applied to various materials, including conductive and non-conductive ones, such as ceramics, metals, polymers, composites, and alloys like steel, aluminum, and titanium. These materials often exhibit superior mechanical properties, making them difficult to cut using conventional methods [3, 4]. As a non-contact process, laser cutting reduces mechanical stress on the material, enhances accuracy, and minimizes tool wear [5, 6]. However, the final quality of laser-cut components is significantly influenced by process parameters, such as laser power (Pu), cutting speed (V), focal position (FP), gas pressure (P), and frequency (F). Several studies have investigated the influence of laser cutting parameters on cut quality: Lopez et al. [7], optimized nozzle focal position and stand-off distance to improve cutting reliability and minimize material waste. Their results showed that a 10 kW fiber laser produced narrower kerfs than previous studies.

Yilbas et al. [8], examined kerf width variations in laser cutting of Ti-6Al-4V, stainless steel 304, Inconel 625, and alumina. Their findings revealed that kerf width increases with higher laser power but decreases with increased cutting speed [8]. Boujelbene et al. [9], evaluated cut quality by measuring heat-affected zone thickness, microhardness, and surface roughness. A predictive model was developed, demonstrating that (Pu) and (V) significantly influence HAZ and microhardness. Nguyen et al. [10], compared Taguchi's design and Response Surface Methodology for optimizing laser cutting settings on stainless steel 304. Cutting speed had the most significant effect on dimensional accuracy, followed by laser

http://doi.org/10.30684/etj.2025.157215.1897
Received 09 February 2025; Received in revised form 07 April 2025; Accepted 17 April 2025; Available online 11 August 2025
2412-0758/University of Technology-Iraq, Baghdad, Iraq

power. Vora et al. [11], investigated the effects of fiber laser cutting parameters on surface roughness (SR), kerf width, dross height, and material removal rate. Gas pressure had the greatest impact, followed by (Pu) and (V). Tura et al. [12], applied response surface techniques and a genetic algorithm to optimize cutting speed, nitrogen pressure, and (FP) for improved SR in CO2 laser cutting. Genna et al. [3], analyzed the influence of material type, thickness, cutting speed, and gas pressure on cut quality using a CO_2 laser. Their study focused on $AlMg_3$ aluminum alloy, St37-2 low-carbon steel, and AISI 304 stainless steel [3]. Anghel et al. [13], investigated the effects of gas pressure (P), frequency (F), cutting speed (V), and laser power (Pu) on surface roughness (SR). ANOVA results indicated that focal position (FP) was the most influential parameter.

While previous research has primarily examined the effects of a limited number of parameters on laser cutting quality, this study provides a more comprehensive analysis by investigating the combined influence of five key parameters laser power, cutting speed, frequency, focal position, and gas pressure—on top and bottom kerf width, backed by robust statistical analysis. This study quantifies the impact of each parameter and establishes optimal cutting conditions to improve precision and efficiency in stainless steel 201 laser cutting. These contributions are a valuable reference for industries seeking to improve laser cutting performance through data-driven optimization strategies.

2. Experimental procedures

2.1 Apparatus and material selection

The experiments were conducted using a fiber laser IGR-3015F IGOLDEN CNC machine with a maximum power of 12000 Watts and a maximum cutting area of 3000 mm × 1500 mm. In all tests, the focal point was consistently set at 10 mm, with a standoff distance of 0.5 mm and a duty cycle of 100%. Compressed air was used as the assist gas.

A circular nozzle with a diameter of 3 mm was used, and oxygen (O_2) was employed as the gas pressure. The air nozzle and the scanner were mounted on a standard three-axis CNC machine center. Consequently, traditional CNC programming was used to program the tests fully. A 5 mm thick stainless steel 201, an austenitic steel, was used as the workpiece material. This material contains high levels of manganese and chromium with a lower percentage of nickel. It is widely employed in various applications due to its unique properties, such as good corrosion resistance and high strength. Applications include the automotive industry, consumer goods, kitchenware, household utensils, and architecture. The tests were conducted on cold-formed sheets that were not coated or treated. Table 1 provides the chemical composition of the material.

Table 1: Chemical composition (wt.%) and the ASM standard for Stainless Steel 201

Element%	Chemical composition	ASM
C	0.136	Max. 0.15
Si	0.219	Max. 1
Mn	5	5.5 - 7.5
P	<0.0005	Max. 0.060
Cr	16	16-18
Mo	<0.002	-
Ni	4.09	3.5-5.5
Cu	0.284	-
Al	<0.001	-

The metal was cut into 32 equally sized samples, each measuring 50×40×5 mm^3, ensuring that the notch previously made by the fiber laser cutting (LC) process was positioned in the middle of each sample as shown in Figure 1a. The notch was produced at a length of 3.5 cm, as shown in Figure 1b.

2.2 Selection of parameters for experimental work

Selecting the optimal set of process parameters is essential to maintaining a high production rate and achieving satisfactory quality for the cut components. In this study, the key controllable process parameters in laser metal cutting selected are cutting speed (V) in m/min, frequency (F) in Hz, focal position (FP) in mm, gas pressure (P) in MPa, and laser power (Pu) in Watts, all at three levels. Some of these parameters significantly impact the final components' unique macroscopic and microscopic properties, which are crucial for evaluating surface finish. Estimates and details are provided in Table 2.

Table 2: Assignment of levels to control factors

Control Variables	Symbol	Unit	Level 1	Level 2	Level 3
Laser Power	Pu	Watt	2000	6000	10000
Cutting speed	V	mm/min	0.5	1	1.5
Assist gas pressure	P	Mpa	7	13	10
Frequency	F	Hz	100	2550	5000
Focus position	FP	mm	-25	-12	1

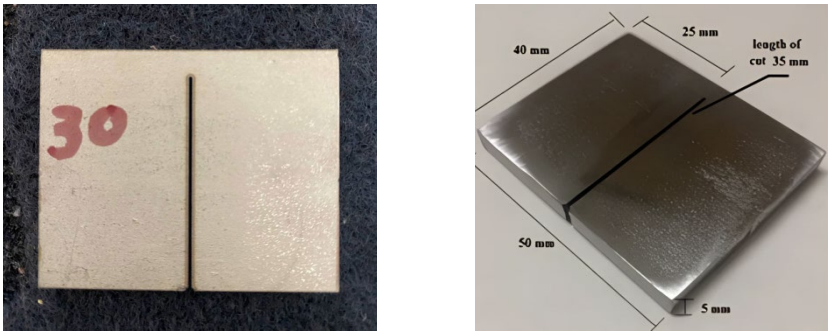

(a) (b)

Figure 1: a) Photograph of the sample with central notch created by fiber laser cutting, b) Sample with dimensional annotations

2.3 Plan of experimentation

To reduce the number of experiments while accurately modeling and optimizing the process, the experimental runs were determined using Minitab V16, a statistical program, in accordance with Response Surface Methodology (RSM) [14].

The current study employed a five-factor, three-level Central Composite Design (CCD) experimental schedule consisting of 26 non-central points and six central points. The experimental plan comprised 32 tests. It was necessary to keep all parameters under strict control. The laser machine was equipped with various measuring devices to examine the interrelationship between the main process parameters thoroughly. Kerf width was among the critical parameters considered before starting the experimental tests. In the laboratory, the KNUTH-SPORT 2 was used for precision grinding and surface preparation, while the DAP-5 was employed for polishing to achieve the required surface finish. Two types of abrasives or diamond pastes (3 µm and 1 µm) and three types of sandpaper (180, 220, and 500 grit) were employed for this purpose.

3. Measurement of the kerf width (KW)

The two quality attributes, top and bottom kerf width, were examined along the cut's length, specifically a 35 mm straight cut on the workpiece. Kerf width was evaluated using the dimensional difference of the cutting edge. The experiments were conducted in the order specified by the Design Expert to avoid introducing random errors into the experimental process. As shown in Figure 2 a the workpiece materials were kept horizontal throughout the entire experiment, TKW and BKW were measured independently using a metallurgical incident light microscope (KRUSS - model MBL3300) at 4X magnification, which provides magnifications up to 1000X, ensuring high-detail observation, accuracy typically falls within ±1 µm as showing in Figure 2 b.

To minimize experimental error, three measurements of the sliced surface were taken. The average of these three measurements was used to determine the TKW and BKW. The measurements, denoted as K1, K2, and K3, were evenly spaced within the stable cutting length of the TKW and BKW, Figure 3 a Schematic Diagram of TKW and BKW Measurement Points whill (b) and (c) show Microscopic Image of the Cut with BKW and TKW Measurement Points, respectively. The scratches observed on the top and bottom of the piece were caused by the polishing process, which proceeded directly to the finishing stage without passing through lower-grit sandpapers, such as 800 and 1000 grit.

Finally, the RSM Method was applied using Minitab® software to organize all measured values and perform statistical analysis, identifying the best set of parameters. The kerf width was determined using Equation 1:

$$\text{Kerf width} = (K1 + K2 + K3) / 3 \quad (1)$$

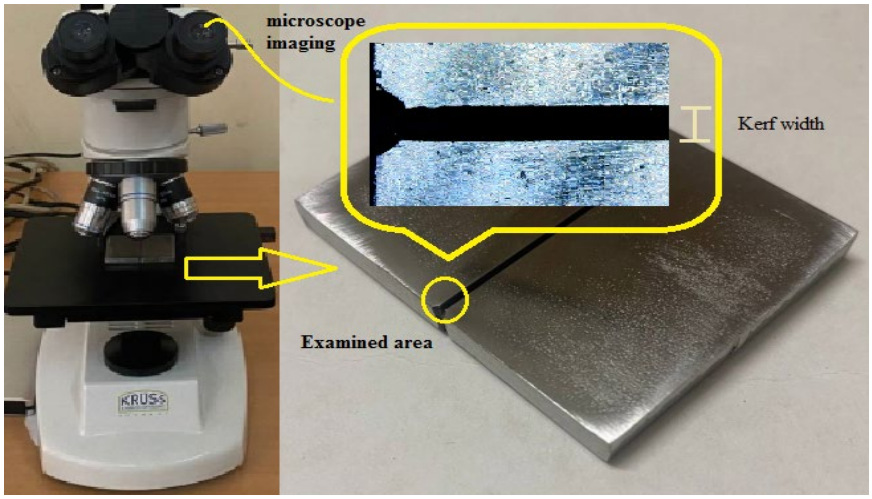

Figure 2: a) General view of the light Microscope b) Definition of kerf geometers

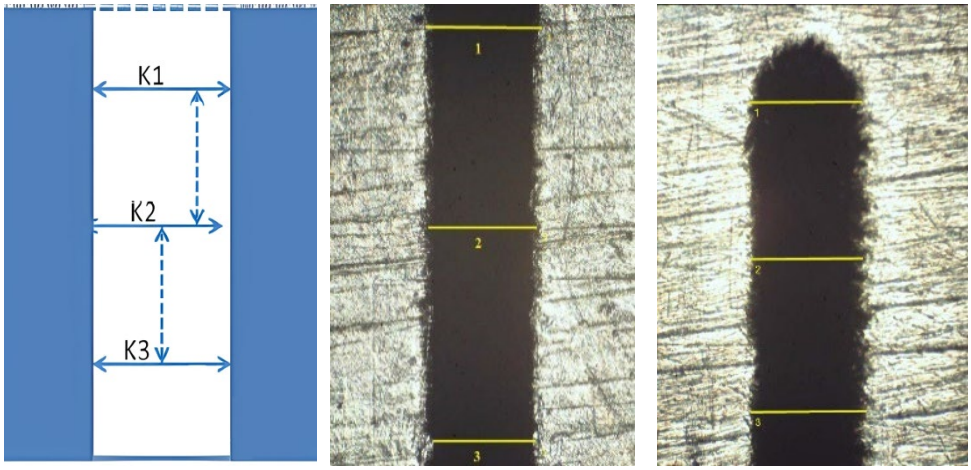

Figure 3: a) Schematic Diagram of TKW and BKW Measurement Points, b) and c) Microscopic Image of the Cut with BKW and TKW Measurement Points respectively

Table 3: Experimental values of TKW and BKW in micrometer based on RSM technique

Control variable in experimental L32						Respons parameter	
Run #	**(Pu) watt**	**(V) mm/min**	**(P) Mpa**	**(F) Hz**	**(FP) mm**	**TKW (µm)**	**BKW (µm)**
1	2000	0.5	13	5000	1	1168.546	531.09
2	2000	0.5	13	100	-25	992.5117	990.51
3	2000	0.5	7	100	1	1197.383	629.22
4	2000	0.5	7	5000	-25	1149.818	912.17
5	2000	1	10	2550	-12	959.5537	765.55
6	2000	1.5	7	100	-25	1131.464	1042.7
7	2000	1.5	7	5000	1	1053.655	694.80
8	2000	1.5	13	100	1	990.8285	634.09
9	2000	1.5	13	5000	-25	735.0224	658.81
10	10000	0.5	13	5000	-25	546.8884	484.65
11	10000	0.5	13	100	1	979.2254	487.40
12	10000	0.5	7	100	-25	635.776	503.34
13	10000	0.5	7	5000	1	928.2819	425.10
14	10000	1	10	2550	-12	605.7	464.80
15	10000	1.5	13	5000	1	843.2652	369.64
16	10000	1.5	13	100	-25	648.693	494.02
17	10000	1.5	7	5000	-25	618.9168	401.10
18	10000	1.5	7	100	1	914.8905	482.03
19	6000	0.5	10	2550	-12	694.014	556.19
20	6000	1.5	10	2550	-12	694.4491	493.64
21	6000	1	10	2550	1	966.22	681.30
22	6000	1	10	5000	-12	507.1217	456.56
23	6000	1	13	2550	-12	652.2535	597.01
24	6000	1	7	2550	-12	643.2014	620.20
25	6000	1	10	2550	-25	788.89	786.40
26	6000	1	10	100	-12	612.9282	578.45
27	6000	1	10	2550	-12	657.9514	609.20
28	6000	1	10	2550	-12	661.3063	599.70
29	6000	1	10	2550	-12	656.7441	614.61
30	6000	1	10	2550	-12	649.3506	617.98
31	6000	1	10	2550	-12	688.2069	595.0
32	6000	1	10	2550	-12	694.014	589.3

4. Analysis of top kerf width

The lowest TKW value is preferred to achieve the best quality. The significance of the selected input variables was analyzed using the Analysis of Variance approach. The ANOVA table for TKW is presented in Table 4. The F-value and p-value were used to evaluate the significance of the input variables. An ANOVA analysis was conducted at a 95% confidence level, where a p-value less than 0.05 indicates that the variable significantly affects the chosen response [15, 16].

As demonstrated in Table 4, TKW is significantly influenced by every machining parameter, including laser power (A), cutting speed (B), assist gas pressure (C), frequency (D), and focal position (E). The difference between the R-squared (R-sq.) and adjusted R-squared (Adj. R-sq.) values were found to be less than 20%, indicating that the model is appropriate [17, 18]. Based on the R-sq. and Adj. R-sq. values for TKW, the model best fits the available data.

Table 4: ANOVA for TKW

Source	DF	Adj SS	Adj MS	F-Value	P-Value	VIF
Liner	5	640837	63140	59.18	0.000	
A	1	392246	392246	367.67	0.000	1.00
B	1	24293	24293	22.77	0.001	1.00
C	1	28493	28493	26.71	0.000	1.00
D	1	16939	16939	15.88	0.002	1.00
E	1	178865	178865	167.66	0.000	1.00
2-Way Interaction	**10**	**122539**	**12254**	**11.49**	**0.000**	
A*B	1	17748	17748	16.64	0.002	1.00
A*C	1	19995	19995	18.74	0.001	1.00
A*D	1	81	81	0.08	0.787	1.00
A*E	1	41391	41391	38.80	0.000	1.00
B*C	1	4797	4797	4.50	0.058	1.00
B*D	1	11218	11218	10.51	0.008	1.00
B*E	1	4897	4897	4.59	0.055	1.00
C*D	1	2225	2225	2.09	0.177	1.00
C*E	1	15657	15657	14.68	0.003	1.00
D*E	1	4530	4530	4.25	0.064	1.00

Model Summary
S=32.6628, R-sq= 99.08%, R-sq(adj)=97.41%, R-sq(pred) 21.90%

Regression Equation in Uncoded Units, Equation 2:

$$TKW = 1416 - 0.1602\ A - 283\ B + 28.8\ C + 0.1206\ D + 25.56\ E + 0.000007\ A\times A + 123.9\ B\times B - 1.72\ C\times C - 0.000017\ D\times D + 1.268\ E\times E + 0.01665\ A\times B + 0.002946\ A\times C - 0.000000\ A\times D + 0.000978\ A\times E - 11.54\ B\times C - 0.02162\ B\times D - 2.69\ B\times E - 0.00160\ C\times D + 0.802\ C\times E + 0.000528\ D\times E \quad (2)$$

Figure 4 displays the residual plots for TKW. Plotting residuals is crucial for validating the ANOVA findings [18]. The four-in-one residual plots include a normal probability plot, a residual vs. fitted value plot, a residual vs. fitted values plot, residuals vs. observation order plot, and a histogram. In the normality test, all residuals align along a straight line, as seen in Figure 4, indicating that they are normally distributed without residual clustering. In the residual versus fitted plot, the residuals are randomly distributed, a key indication of effective statistical analysis in ANOVA. The histogram exhibits a parabolic shape, further confirming the normality of the data. When no discernible trend is observed in the residual vs. fitted values plot, the ANOVA findings are considered a good fit. These results confirm that all four tests validate the proposed model, suggesting that future predictions will be reliable. Additionally, the effects of two simultaneous input variables on TKW were analyzed using contour plots, keeping the third input variable constant.

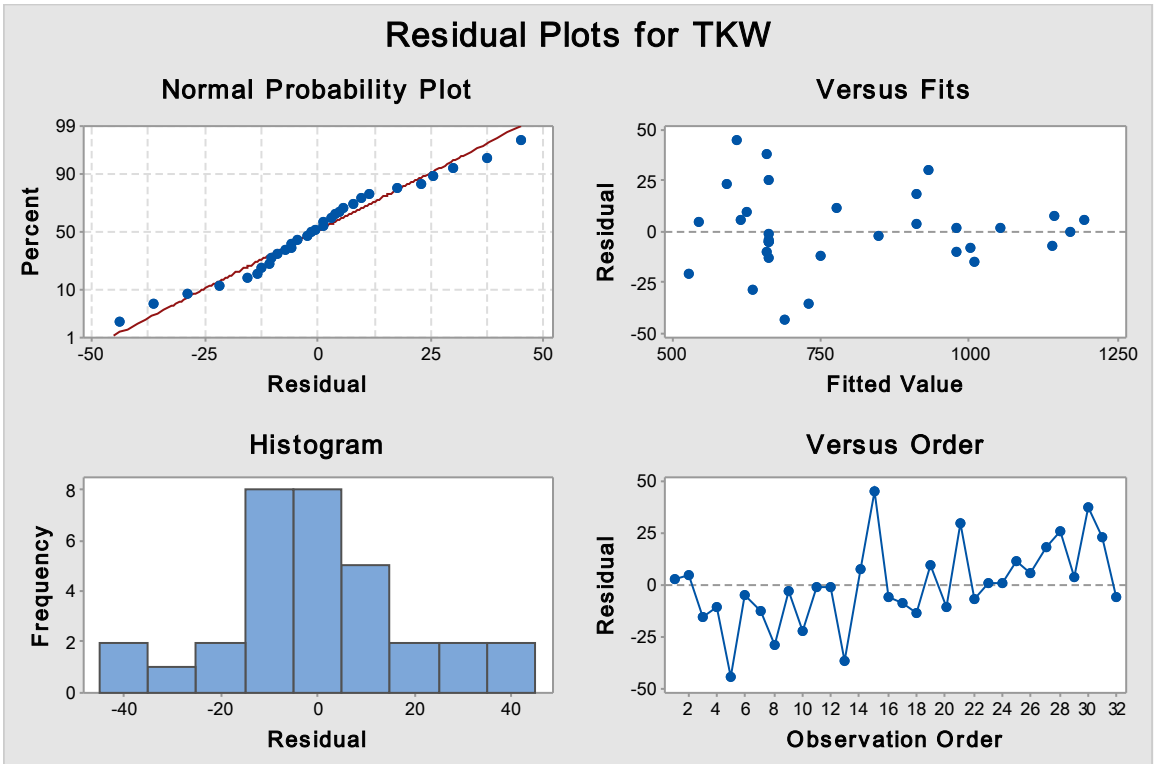

Figure 4: Residual plots for TKW

The ANOVA results for TKW revealed that all five machining parameters-laser power (Pu), cutting speed (V), gas pressure (P), frequency (F), and focal position (FP)-had a statistically significant impact on TKW. Among these, Pu was the most influential parameter, contributing 61% to the variation in TKW, followed by FP at 19.8%, P at 4.5%, V at 3.8%, and F at 2.7%. A pie chart representing the proportional contribution of machining factors to TKW is displayed in Figure 5. The standard deviation of TKW was 32.6628, indicating a maximum deviation of 32.6628 from the mean TKW value.

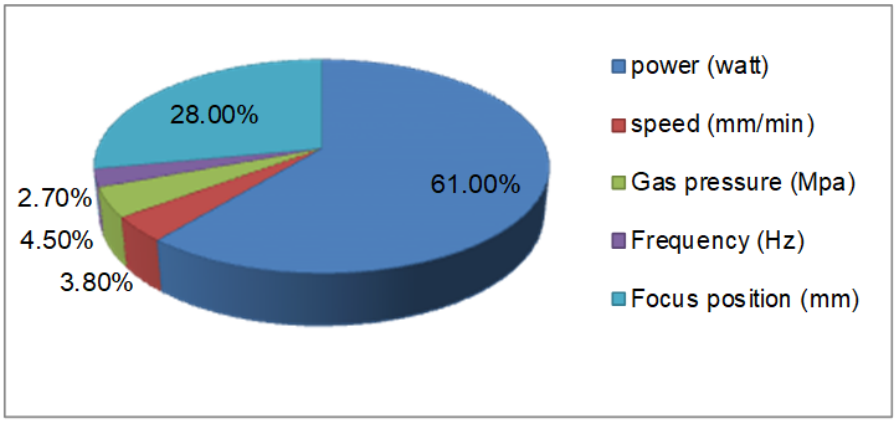

Figure 5: The percentage that machining factors contribute to TKW

Figure 6 displays the effect of machining factors on TKW based on the main effect plot. The main effect graphs depict the mean response of each level of the parameters connected by a line. The Y-axis represents the mean TKW values achieved for various levels of input machining parameters. The results showed that increasing laser power led to a significant reduction in TKW. This can be attributed to the higher energy density at increased power levels, which enhances material removal efficiency and results in a narrower kerf. This finding aligns with the work of Yilbas et al. [8], who reported that higher laser power reduces kerf width due to increased melting and vaporization of the material.

Similarly, focal position played a critical role in determining TKW. The optimal focal position was approximately -12 mm, which minimizes TKW. This finding is consistent with Lopez et al. [7], who emphasized the importance of precise focal positioning to achieve minimal kerf width and improved cutting quality. Increasing gas pressure resulted in a continuous decrease in TKW. Higher gas pressure enhances the ejection of molten material from the cutting zone, reducing material re-deposition and dross formation. Vora et al. [11], support this observation, noting that gas pressure significantly affects kerf width and surface quality. While cutting speed and frequency had relatively lower contributions to TKW, their effects were still significant. Cutting speed showed a relatively constant effect within the 1 to 1.5 mm/min range, suggesting that speed variations did not drastically alter TKW. This aligns with Nguyen et al. [10], who reported that cutting speed has a moderate impact on kerf width compared to other parameters. On the other hand, frequency exhibited a parabolic curve, indicating an optimal frequency level for minimizing TKW. This behavior can be explained by the balance between energy input and material removal efficiency at different frequencies.

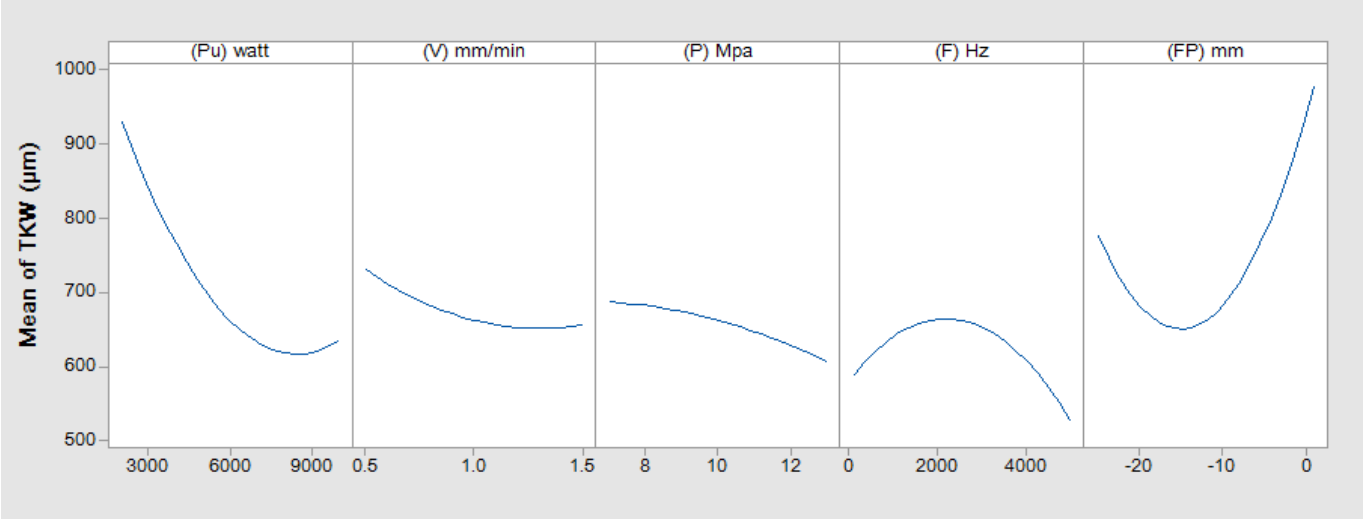

Figure 6: Effects of the machining parameters on TKW

5. Analysis of bottom kerf width

In the same way, Table 5 indicates that all of the machining factors significantly impact BKW.

Table 5: ANOVA for BKW

Source	DF	Adj SS	Adj MS	F-Value	P-Value	VIF
Liner	5	579951	115990	392.89	0.000	
A	1	419180	419180	1419.87	0.000	1.00
B	1	3440	3440	11.65	0.006	1.00
C	1	11932	11932	40.42	0.000	1.00
D	1	45787	45787	155.09	0.000	1.00
E	1	99611	99611	337.41	0.000	1.00
2-Way Interaction	**10**	**125581**	**12558**	**42.54**	**0.000**	
A*B	1	917	917	3.11	0.106	1.00
A*C	1	14916	14916	50.53	0.000	1.00
A*D	1	2845	2845	9.64	0.010	1.00
A*E	1	62007	62007	210.03	0.000	1.00
B*C	1	14877	14877	50.39	0.000	1.00
B*D	1	4591	4591	15.55	0.002	1.00
B*E	1	10090	10090	34.18	0.000	1.00
C*D	1	7128	7128	24.14	0.000	1.00
C*E	1	31	31	0.11	0.751	1.00
D*E	1	8178	8178	27.70	0.000	1.00

Model Summary
S=17.1821, R-sq=99.58%, R-sq(adj)=98.81%, R-sq(pred)=70.22%

Regression Equation in Uncoded Units, Equation 3:

$$BKW(\mu m) = 490 - 0.06141\ A + 868.7\ B - 18.2\ C + 0.0911\ D + 0.28\ E + 0.000001\ A\times A - 294.4\ B\times B + 1.12\ C\times C$$
$$0.000013\ D\times D + 0.8008\ E\times E - 0.00378\ A\times B + 0.002544 A\times C + 0.000001 A\times D + 0.001197 A\times E - 20.33 B\times C - 0.01383 B\times D$$
$$+ 3.863\ B\times E - 0.002872\ C\times D + 0.036\ C\times E + 0.000710\ D\times E \quad (3)$$

Figure 7 displays the residual plots for BKW. The results indicate that all residuals are normally distributed, with no evidence of clustering. The normality of the data is further supported by the residual versus fitted values plot, which exhibits a random distribution of residuals without a clear parabolic trend. This confirms that all four tests validate the proposed model, suggesting that future results will be reliable.

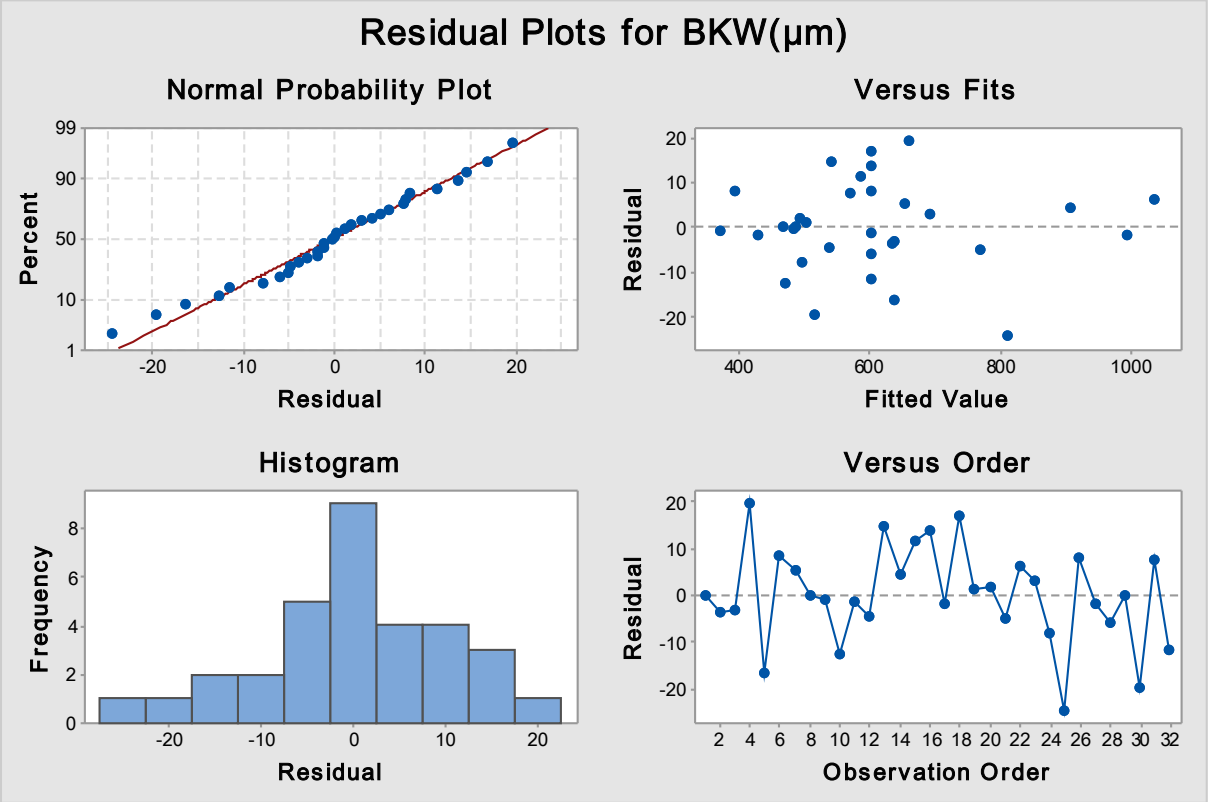

Figure 7: Residual plots for BKW

The ANOVA results for BKW indicated that all five machining parameters significantly influenced BKW. Laser power was the most dominant factor, contributing 72% of the variation in BKW, followed by focal position at 17%, frequency at 8%,

gas pressure at 2%, and cutting speed at 1%. Figure 8 displays a pie chart illustrating the proportional contribution of machining factors to BKW.

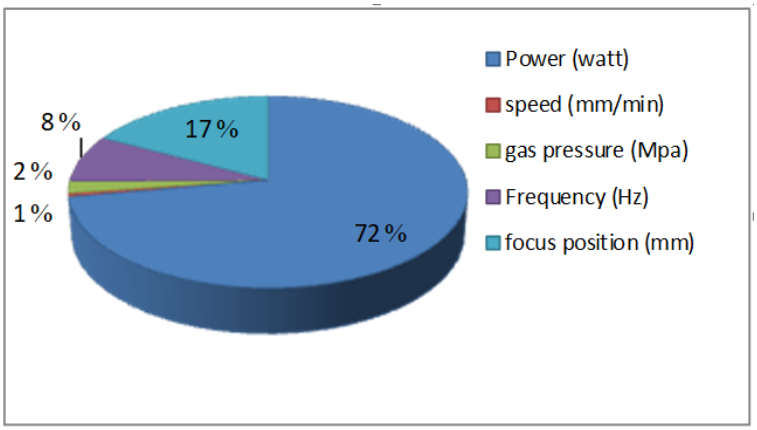

Figure 8: contribution of machining variables as a percentage of BKW

Figure 9 displays the effect of machining factors on BKW based on the main effect plot. The main effect graphs show the average response at each level of the parameters, connected by a line. The Y-axis represents the mean BKW values achieved for various levels of input machining parameters. The strong influence of laser power on BKW can be attributed to the same mechanisms as TKW. Higher power levels result in more efficient material removal, leading to a narrower kerf at the bottom of the cut. This finding aligns with Boujelbene et al. [9], who reported that laser power significantly affects the kerf geometry, especially in thicker materials.

Similarly, the focal position had a notable impact on BKW, with the optimal position found to be approximately -12 mm, where the kerf width was minimized. This finding is consistent with Genna et al. [3], who emphasized the importance of focal position in controlling kerf width and ensuring uniform cutting quality throughout the material thickness.

Frequency exhibited a non-linear effect on BKW, with an optimal point around 2000 Hz where the kerf width was minimized. This behavior mirrors that observed for TKW and can be explained by the interaction between laser pulses and the material. At lower frequencies, the energy input may be insufficient for efficient material removal, while at higher frequencies, excessive energy input can lead to increased kerf width due to thermal effects. Gas pressure and cutting speed had relatively lower contributions to BKW than laser power and focal position. However, their effects were still significant, with higher gas pressure reducing BKW due to improved melt ejection. Cutting speed exhibited a U-shaped effect, where the lowest BKW values were observed at the two extreme cutting speed levels tested. This finding agrees with Kotadiya et al. [4], who reported that cutting speed has a moderate impact on kerf width, especially in thinner materials.

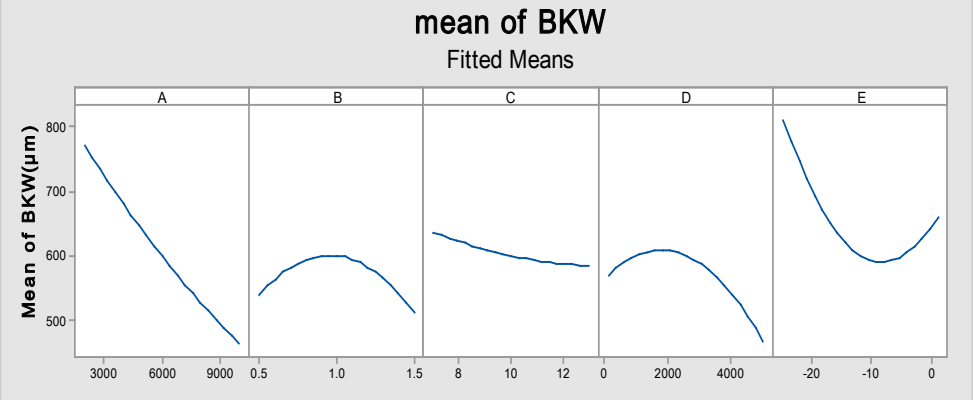

Figure 9: Impact of machining variables on BKW

The stronger influence of laser power on BKW (72%) compared to TKW (61%) can be attributed to how heat supply affects the machining zone. As laser power increases, TKW gradually decreases until it reaches a relative stabilization. This suggests that increasing Pu enhances performance to a certain level, beyond which the effect becomes negligible.

This phenomenon occurs due to the heat accumulation in the machining zone. When the heat supply is lower, the molten material becomes more viscous and difficult to remove, increasing the bottom kerf width. Therefore, the greater sensitivity of the bottom region to heat accumulation and material flow behavior explains the stronger influence of laser power on BKW compared to TKW [19, 20].

6. Interaction effects

Figures 10 and 11 display the interaction plots, highlighting key relationships between the machining parameters. For both top kerf width and bottom kerf width, the strongest interactions were observed between gas pressure and cutting speed, as well

as between focal position and gas pressure. These interactions indicate that P's effects on kerf width depend highly on V and FP. For example, increasing P had a more pronounced effect on reducing kerf width at higher V. This finding aligns with the work of Tura et al. [12], who reported similar interactions in their study on laser cutting of SST.

Conversely, the interactions between laser power and frequency and between laser power and focal position were relatively weaker. This suggests that while Pu is the dominant factor, its effect on kerf width is less influenced by the frequency and focal position levels. This observation is supported by Anghel et al. [13], who noted that laser power has a more independent effect on kerf width compared to other machining parameters.

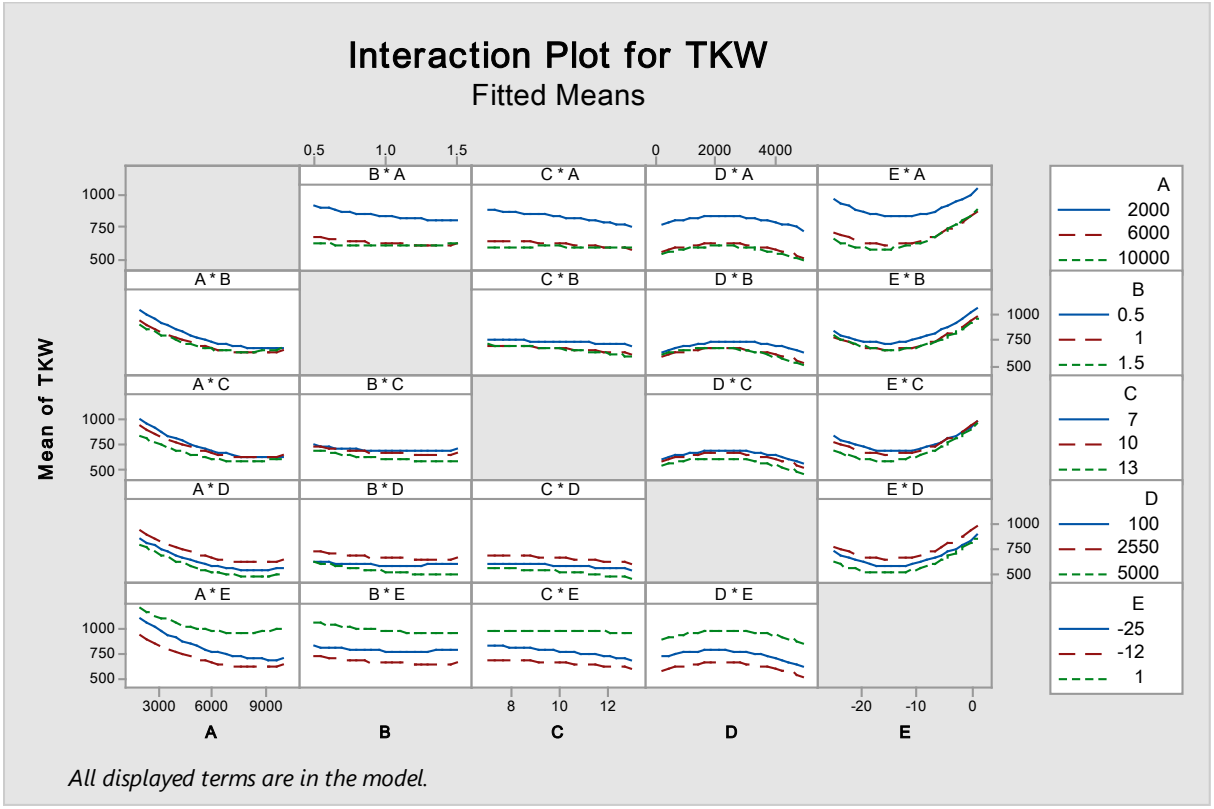

Figure 10: Interaction Plot illustrates the relationship between each factor

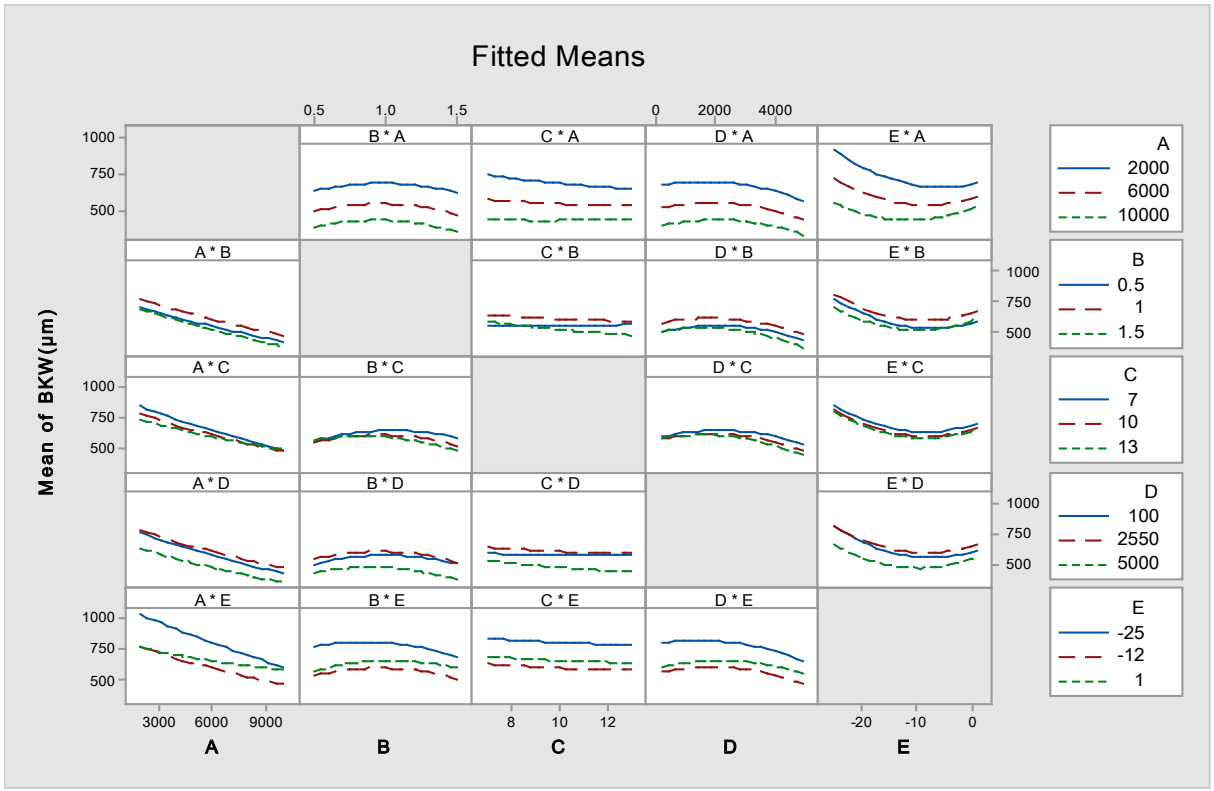

Figure 11: Interaction Plot illustrates the relationship between each factor

The results of this study align well with previous research on laser cutting of SST and other materials. For instance, Yilbas et al. [8], and Nguyen et al. [10], reported that Pu and V are critical factors in determining kerf width. However, the current study provides a more comprehensive analysis by incorporating additional parameters, such as frequency and focal position, which were found to have significant but previously underreported effects on kerf width.

Furthermore, the findings emphasize the crucial role of gas pressure and focal position in controlling kerf width, consistent with the work of Lopez et al. [7], and Genna et al., [3]. However, this study extends previous research by quantifying the contributions of these parameters and identifying optimal levels for minimizing kerf width.

7. Conclusion

This study analyzed the effects of fiber laser cutting parameters on the kerf width of stainless steel 201—p, F, Pu, V, and FP. The TKW and BKW were examined as response variables using statistical methods, including ANOVA and interaction analysis. The developed regression models demonstrated high accuracy, providing a reliable tool for optimizing laser cutting processes. These findings enhance the understanding of parameter interactions and contribute to improving precision in industrial laser-cutting applications. The key conclusions from this study are as follows:

1) All five machining variables were significant based on the ANOVA results for TKW. Laser power had the largest contribution at 61%, followed by focal position (19.8%), gas pressure (4.5%), cutting speed (3.8%), and frequency (2.7%).
2) Similarly, all five machining variables were significant for BKW, with Laser power contributing the most (72%), followed by focal position (17%), frequency (8%), gas pressure (2%), and cutting speed (1%).
3) Interaction plots revealed the significance of parameter interactions. The strongest interactions were observed between gas pressure and cutting speed and between gas pressure and focal position. Weaker interactions were found between laser power and frequency and between laser power and focal position. Moderate interactions were observed between the focal position and gas pressure and between the focal position and cutting speed.
4) The findings are consistent with previous research while offering new insights into the interactions between these parameters.
5) The regression models developed in this study can be used to optimize laser cutting processes and improve cutting quality in industrial applications.
6) All response models showed an R-squared (R-sq.) and adjusted R-squared (Adj. R-sq.) difference of less than 20%, confirming that the proposed models provide an excellent fit to the experimental data.

8. Limitations of the study

The findings of this study are limited to the specific range of laser-cutting parameters and materials investigated. The experiments were conducted using a fixed set of process parameters—laser power, cutting speed, gas pressure, frequency, and focal position—within predefined levels. Consequently, conclusions may not directly apply to other parameter settings or material types.

Additionally, the dataset used for analysis was constrained to the selected experimental design, which may not capture all possible interactions between variables. To improve the generalizability of the results, further studies should explore a broader range of parameters and additional material compositions. Future research can also incorporate alternative experimental techniques and advanced statistical models to refine the understanding of laser cutting effects on kerf width and heat-affected zones.

9. Future research directions

integrating machine learning models or finite element analysis (FEA) could enhance process prediction and control by establishing more precise relationships between laser parameters and kerf quality. Future studies may also investigate the effects of different assist gases, such as argon or air, and multi-pass cutting strategies to assess their influence on cutting efficiency and material integrity. Additionally, conducting industrial-scale experiments with automated CNC systems could validate the research findings under real manufacturing conditions, ensuring broader applicability in precision machining and sheet metal processing industries.

Nomenclature

ANOVA	Analysis of variance.	P	Assist gas pressure, bar.
BKW	Bottom kerf width (μm).	Pu	Laser power, W.
CNC	Computer Numerical Control.	RSM	Response Surface Methodology.
F	Pulse frequency, Hz.	SR	Surface roughness.
FP	Focal position, mm.	SS	Stainless steel.
HAZ	heat effect zone.	SOD	Standoff distance.
LC	Laser cutting.	TKW	Top kerf width (μm).
MRR	material removal rate.	V	Cutting speed, mm/min.
O_2	Oxygen gas.	W.P	Workpiece.

Author contributions

Conceptualization, **A. Zabon**, **T. Abbas**, and **A. Bedan**; data curation, **A. Zabon**; formal analysis, **A. Zabon**; investigation, **A. Zabon**; methodology, **A. Zabon**.; project administration, **A. Zabon**, resources, **A. Zabon**; software, **A. Zabon**; supervision, **T. Abbas**. and **A. Bedan**; validation, **T. Abbas**, **A. Bedan**; visualization, **T. Abbas**, **A. Bedan**; writing—original draft preparation, **A. Zabon**; writing—review and editing, **T. Abbas**, **A. Bedan**. All authors have read and agreed to the published version of the manuscript.

Funding

This research received no specific grant from any funding agency in the public, commercial, or not-for-profit sectors.

Data availability statement

The data that support the findings of this study are available on request from the corresponding author.

Conflicts of interest

The authors declare that there is no conflict of interest.

References

[1] S. B. Abd Halim, Performance evaluation of nitrogen gas-assisted laser cutting on 316L ASS plate, thesis Faculty of Mechanical Engineering Universiti Teknologi Malaysia. May, 2010.

[2] Y. A. Turkkan, M. Aslan, A. Tarkan, Ö. Aslan, C. Yuce, and N. Yavuz, Multi-Objective Optimization of Fiber Laser Cutting of Stainless-Steel Plates Using Taguchi-Based Grey Relational Analysis, Metals (Basel)., 13 (2023) 132. http://dx.doi.org/10.3390/met13010132

[3] S. Genna, E. Menna, G. Rubino, and V. Tagliaferri, Experimental investigation of industrial laser cutting: The effect of the material selection and the process parameters on the kerf quality, Appl. Sci., 10 (2020) 4956. http://dx.doi.org/10.3390/app10144956

[4] D. J. Kotadiya, J. M. Kapopara, A. R. Patel, C. G. Dalwadi, and D. H. Pandya, Parametric analysis of process parameter for Laser cutting process on SS-304, Mater. Today Proc., 5 (2018) 5384-5390. https://doi.org/10.1016/j.matpr.2017.12.124

[5] H. M. A. Elsayed, Modeling and optimization of laser cutting operations, Minia University Faculty of Engineering Production Eng. & Design Department, Manuf. Rev., 2 (2015). https://doi.org/10.1051/mfreview/2015020

[6] A. S. Bedan, K. K. Mansor, K. K. Anwer, and H. H. Kadhim, Design and Implementation of Asymmetric Extrusion Die Using Bezier Technique, IOP Conference Series: Materials Science and Engineering, 881 (2020) 01252. https://doi.org/10.1088/1757-899X/881/1/012052

[7] A. B. Lopez, E. Assunção, L. Quintino, J. Blackburn, and A. Khan, High-power fiber laser cutting parameter optimization for nuclear Decommissioning, Nucl. Eng. Technol., 49 (2017) 865-872. https://doi.org/10.1016/j.net.2017.02.004

[8] B. S. Yilbas, M. M. Shaukat, and F. Ashraf, Laser cutting of various materials: Kerf width size analysis and life cycle assessment of cutting process, Opt. Laser Technol., 93 (2017) 67-73. https://doi.org/10.1016/j.optlastec.2017.02.014

[9] M. Boujelbene, A. S. Alghamdi, I. Miraoui, E. Bayraktar, and M. Gazbar, Effects of the laser cutting parameters on the micro-hardness and on the heat affected zone of the mi-hardened steel, Int. J. Adv. Appl. Sci., 4 (2017) 19-25. http://dx.doi.org/10.21833/ijaas.2017.05.003

[10] V. Nguyen, F. Altarazi, and T. Tran, Optimization of Process Parameters for Laser Cutting Process of Stainless Steel 304: A Comparative Analysis and Estimation with Taguchi Method and Response Surface Methodology, Math. Probl. Eng., 2022 (2022) 6677586. https://doi.org/10.1155/2022/6677586

[11] J. Vora, R. Chaudhari, C. Patel, D. Y. Pimenov, V. K. Patel, Kh. Giasin and S. Sharma, Experimental investigations and pareto optimization of fiber laser cutting process of Ti6AL4V, Metals (Basel)., 11 (2021) 1-27. https://www.mdpi.com/2075-4701/11/9/1461

[12] A. D. Tura, H. B. Mamo, and D. G. Desisa, Multi-objective optimization and analysis for laser beam cutting of stainless steel (SS304) using hybrid statistical tools GA-RSM, IOP Conference Series: Materials Science and Engineering,1201 (2021) 012030. https://doi.org/10.1088/1757-899x/1201/1/012030

[13] C. Anghel, K. Gupta, and T. C. Jen, Analysis and optimization of surface quality of stainless steel miniature gears manufactured by CO2 laser cutting, Optik (Stuttg), 203 (2020) 164049. https://doi.org/10.1016/j.ijleo.2019.164049

[14] M. Li, Evaluation of the effect of process parameters on the cut quality in fiber laser cutting of duplex stainless steel using response surface method (RSM), Infrared Phys. Technol., 118 (2021) 103896. https://doi.org/10.1016/j.infrared.2021.103896

[15] A. Chaurasia, V. Wankhede and R. Chaudhari, Experimental Investigation of High-Speed Turning of INCONEL 718 Using PVD-Coated Carbide Tool Under Wet Condition, 757 (2019) 367-374. http://dx.doi.org/10.1007/978-981-13-1966-2_32

[16] K. K. mansor, A. H.shabeb, E. A. Hussein,T. F. Abbas and A. S. Bedan, A Statistical Investigation and Prediction of the Effect of FDM Variables on Flexural Stress of PLA Prints, Tikrit J. Eng. sci., 31 (2024) 10-17. https://doi.org/10.25130/tjes.31.3.2

[17] R. Chaudhari, J. J. Vora, L.N. L. de Lacalle, S. Khanna, V. K. Patel and I. Ayesta, Parametric Optimization and Effect of Nano-Graphene Mixed Dielectric Fluid on Performance of Wire Electrical Discharge Machining Process of Ni55.8Ti Shape Memory Allo, Spark Eros. Mach., 14 (2020) 190-216. https://www.mdpi.com/1996-1944/14/10/2533

[18] R. Chaudhari , J. J. Vora, V. Patel, L. N. L. de Lacalle and D. M. Parikh, Surface Analysis of Wire-Electrical-Discharge-Machining-Processed Shape-Memory Alloys, MDPi, 2 (2020) 6-9. https://www.mdpi.com/1996-1944/13/3/530

[19] B. T. Rao, R. Kaul, P. Tiwari, and A. K. Nath, Inert gas cutting of titanium sheet with pulsed mode CO_2 laser, Opt. Lasers Eng., 43 (2005) 1330-1348. https://doi.org/10.1016/j.optlaseng.2004.12.009

[20] D. Scintilla and L. Tricarico, Fusion cutting of aluminum, magnesium, and titanium alloys using high-power fiber laser, Opt. Eng., 52 (2013) 076115. https://doi.org/10.1117/1.OE.52.7.076115